Structural Insights into the Polymorphism of Bismuth(III) Di-*n*-Butyldithiocarbamate by X-Ray Diffraction, Solid-State (^{13}C/^{15}N) CP-MAS NMR, and DFT Calculations

Vasantha Gowda,[a,b,]* Bipul Sarma,[c] Risto S. Laitinen,[d] Anna-Carin Larsson,[a] Alexander V. Ivanov,[e] Dinu Iuga,[f] Perttu Lantto,[b] Oleg N. Antzutkin[a,f,]*

[a] Chemistry of Interfaces, Luleå University of Technology, SE-97187 Luleå, Sweden

[b] NMR Research Unit, University of Oulu, P.O. Box 3000, FI-90014 Oulu, Finland

[c] Department of Chemical Sciences, Tezpur University, 784028, Tezpur, Assam, India

[d] Laboratory of Inorganic Chemistry, University of Oulu, P.O. Box 3000, FI-90014, Finland

[e] Institute of Geology and Nature Management, Far Eastern Branch of the Russian Academy of Sciences, Blagoveshchensk, 675000, Russia

[f] Department of Physics, Warwick University, Coventry CV4 7AL, UK

[*]Email address: gowda.vasantha.k@gmail.com (Vasantha Gowda); Oleg.Antzutkin@ltu.se and O.N.Antzutkin@warwick.ac.uk (Oleg N. Antzutkin)

ABSTRACT

Two crystalline polymorphs of a binuclear tris(di-*n*-butyldithiocarbamato)bismuth(III) complex, I and II, with an empirical formula of [Bi{S$_2$CN(*n*-C$_4$H$_9$)$_2$}$_3$] were synthesised and characterised by X-ray diffraction (XRD), solid-state NMR, and density functional theory (DFT) calculations. At the supramolecular level, these mononuclear molecular units interact in pairs via secondary Bi···S bonds yielding binuclear formations of [Bi$_2${S$_2$CN(*n*-C$_4$H$_9$)$_2$}$_6$]. The polymorph I ($P\overline{1}$) contains two isomeric non-centrosymmetric binuclear molecules of [Bi$_2${S$_2$CN(*n*-C$_4$H$_9$)$_2$}$_6$], which are related to each other as conformers, therefore, having four structurally inequivalent bismuth atoms and twelve inequivalent dithiocarbamate ligands. In contrast, the structurally simpler polymorph II ($P2_1/n$) exists as a single molecular form of the corresponding centrosymmetric binuclear formation comprising two structurally equivalent bismuth atoms and three structurally different dithiocarbamate groups. The polymorphs I and II were found to be interconvertible by altering the solvent system during the recrystallisation process. Sun *et al*. (2012) has reported a crystalline form of the title compound which resembles, but is not identical with, the polymorph II. Experimental solid-state ^{13}C and ^{15}N cross-polarisation (CP) magic-angle-spinning (MAS) NMR spectra of both polymorphs I and II were in accord with the direct structural data on these complexes. Assignments of resonance lines in solid-state ^{13}C and ^{15}N NMR spectra assisted by chemical shift calculations of the crystals using periodic DFT.

Keywords: Bismuth(III) di-*n*-butyldithiocarbamate; Polymorphism; Single-crystal X-ray structure; ^{13}C and ^{15}N CP-MAS NMR; Density functional theory calculations.

1. Introduction

Bismuth (Bi) is the heaviest among the pnictogen (Group 15) elements and it is called 'green' metal, because known bismuth compounds are benign or are considerably less toxic compared to other pnictogens, such as antimony and arsenic [1,2]. Moreover, bismuth compounds may even provide therapeutic responses and antibacterial activities [3]. Metal dithiocarbamate compounds find wide-ranging applications including synthesis of nanomaterials [4,5], solvent extraction of rare earths [6], as additives to lubricating oils [7], as anticarcinogenic drugs [8,9], and as pesticides or fungicides [10-12]. Dithiocarbamates are highly versatile mono-anionic ligands, which can form stable complexes with almost all metals in the periodic table [13]. The metal-dithiocarbamate complexes show a wide structural diversity ranging from mononuclear and binuclear to polymeric supramolecular assemblies [14-16], depending on several factors such as the metal centre, alkyl substituents at the nitrogen atom, and also on solvent properties.

The intermolecular interactions such as van der Waals, secondary and hydrogen bonding, steric repulsions or the weak cooperative interactions like C–H···O hydrogen bonding, $\pi \cdots \pi$, C–H···π, mono- and polyhapta, M···H–C agostic (attractive) and anagostic (repulsive) interactions can play a vital role in stabilising one particular molecular arrangement in a crystal. Because of such weak interactions, various molecular arrangements can have nearly the same energy and the molecules can crystallise in different forms at different experimental conditions such as temperature, solvent properties, solute concentration, crystal growth rate, and a presence of impurities. Different polymorphic forms of a given compound can exhibit differences in solubility, melting point, density, optical and electrical properties, etc. Being able to distinguish different polymorphs and their individual properties is of utmost importance because of their various pharmaceutical applications [17]. Solid-state ^{13}C/^{15}N cross-polarisation (CP) magic-angle-spinning (MAS) NMR spectroscopy

has proven itself as a powerful structural tool for studies of polycrystalline polymorphic systems [18,19]. In solids NMR (^{13}C, ^{15}N, etc.), depending on the number of inequivalent molecules in the asymmetric unit of the crystal structure, one can often observe multiple resonance lines for each symmetrically inequivalent atom. Since different polymorphs of a compound are packed differently in 3-dimensional space, the NMR resonance lines for the symmetrically inequivalent nuclei will differ in different solid polymorphs [20].

In this work, we apply the so called "SMARTER Crystallography" approach [21-26], which enables the combination of experimental solid-state NMR and XRD techniques with theoretical calculations of structure and NMR chemical shifts of periodic systems, aiming to gain much greater insights into the structure and properties of materials, than by any individual approach considered alone. In our previous reports, we have successfully used a similar multidisciplinary approach for structural investigations of the yttrium(III) [27] and lanthanum(III) [28] complexes with diethyldithiocarbamate and phenanthroline ligands.

It has been previously reported by Sun et al. [29] that recrystallisation of the tris(di-n-butyldithiocarbamato)bismuth(III) compound from acetonitrile resulted in monoclinic single crystals ($P2_1/c$), having a centrosymmetric binuclear molecule of $[Bi_2\{S_2CN(n\text{-}C_4H_9)_2\}_6]$ and, therefore, three inequivalent dithiocarbamate ligands in the unit cell. In our case, a comparatively different PXRD pattern and a missing correlation with solid-state ^{13}C/^{15}N NMR spectra for the polycrystalline material of the title compound, also recrystallised from acetonitrile, indicated a different crystal structure type. On the contrary, a recrystallisation from dichloromethane of the title compound resulted in a crystalline form of the compound which showed a good correlation to, in terms of a PXRD pattern and solid-state NMR spectral data, the crystal structure by Sun et al. [29]. Herein, we report synthesis and characterisation of two crystalline polymorphs of tris(di-n-butyldithiocarbamato)bismuth(III) complex, which were obtained by recrystallisation of the synthesised title compound from (i)

acetonitrile (polymorph I) and (ii) dichloromethane (polymorph II), by solid-state ^{13}C and ^{15}N NMR spectroscopy, powder and single crystal XRD, and further explored by employing first principles DFT calculations using gauge including projector augmented wave (GIPAW) method for NMR shieldings. The polymorph I crystallises in the triclinic system ($P\bar{1}$ space group), having four structurally inequivalent mononuclear [Bi{S$_2$CN(n-C$_4$H$_9$)$_2$}$_3$] units, which form two non-centrosymmetric isomeric molecules of [Bi$_2${S$_2$CN(n-C$_4$H$_9$)$_2$}$_6$] stabilised in pairs via non-symmetric secondary Bi⋯S bonds. These binuclear molecules are related to each other as conformational isomers (conformers). The crystal structure of polymorph II was solved and refined in the setting of a monoclinic system with space group $P2_1/n$, which presents significant differences in the bond parameters, especially, for the alkyl chains when compared to the structure by Sun *et al*. (hereafter II^s) [29]. The polymorph II (as for II^s) is also presented by the single centrosymmetric binuclear molecule of [Bi$_2${S$_2$CN(n-C$_4$H$_9$)$_2$}$_6$]: there are two such crystallographically independent molecules per unit cell. Single-crystal structures and experimental solid-state ^{13}C and ^{15}N CP-MAS NMR spectra of I and II were compared with DFT/GIPAW [30-32] calculated structural parameters and chemical shifts.

2. Materials and Methods

Dibutylamine, carbon disulphide, sodium hydroxide, ethanol, dichloromethane, diethyl ether, acetonitrile, and bismuth trinitrate pentahydrate were purchased from Sigma-Aldrich and used without further purification.

2.1. Synthesis of a sodium salt of di-n-butyldithiocarbamate

Sodium di-*n*-butyldithiocarbamate was obtained by the reaction of dibutylamine with carbon disulphide in an alkaline medium at a temperature below 5 °C. In short, di-*n*-butylamine (100 mmol) and sodium hydroxide (100 mmol) were dissolved in ethanol (100 mL) and stirred at 0 °C. Carbon disulphide (101 mmol) was added drop wise to the above stirred mixture. Stirring

was continued for another 2 hours for completion of the reaction. The solvent was evaporated in a rotary evaporator at low pressure. The crude product was washed with diethyl ether and recrystallised from ethanol. The yield was 90%.

2.2. Synthesis of tris(di-n-butyldithiocarbamato)bismuth(III) complex

Bismuth trinitrate pentahydrate [Bi(NO$_3$)$_3$·5H$_2$O] (4.85 g, 10 mmol) was stirred for about 1 hour in 50 mL ethanol, a curdy white solution was obtained. A solution of the sodium salt of di-*n*-dibutyldithiocarbamate (31 mmol) in ethanol was then added and the reaction mixture was stirred for about 4 hours at room temperature. The resulting solution was suction washed with ethanol, filtered, and dried. The yield was 80 %.

In contrast to the previously reported synthetic method by Sun *et al*. [29], the title compound was crystallised in the triclinic system ($P\bar{1}$) upon recrystallisation from acetonitrile at room temperature over a few days (polymorph I). Polymorph II was prepared by the recrystallisation of the dried crude product from dichloromethane. It was also found by NMR and PXRD that polymorph I can be readily converted into polymorph II by switching the recrystallisation solvent from acetonitrile to dichloromethane and *vice versa*.

Melting point: Polymorph I 101-102 °C and polymorph II 96-97 °C.

2.3. Powder X-ray diffraction (PXRD)

The PXRD patterns [see Fig. 1] were collected using a PANalytical Empyrean X-ray diffraction spectrometer (45 kV and 40 mA) and Cu Kα radiation with λ = 1.54 Å. The data collection was performed at ambient room temperature over the range 2θ = 4-40° with a scan interval of θ = 0.013°. The theoretical PXRD patterns of both polymorphs I, and II [see Fig. 1] were calculated using Mercury crystal structure visualisation software (version 3.5) [33].

2.4. Solution-state NMR of [Bi{S$_2$CN(-n-C$_4$H$_9$)$_2$}$_3$]

One-dimensional ^{1}H and ^{13}C (^{1}H decoupled) NMR spectra were measured on a Bruker Avance III spectrometer operating at 400.13 and 100.61 MHz for ^{1}H and ^{13}C, respectively. The spectral parameters for ^{1}H/^{13}C experiments were as follows: $\pi/2$ pulse lengths 8.8/12.0 μs, recycle delay 3/5 s, number of transients 32/1024. Both ^{1}H and ^{13}C spectra were referenced to TMS (0.0 ppm).

^{1}H NMR (solution in CDCl$_3$, see Fig. S1a in ESI): 3.72 ppm (-N-**CH$_2$**-), 1.74 ppm (-**CH$_2$**-), 1.35 ppm (-**CH$_2$**-), and 0.94 ppm (-**CH$_3$**).

^{13}C NMR (solution in CDCl$_3$, see Fig. S1b in ESI): 200.95 ppm (-S$_2$**C**N), 54.32 ppm (-N-**CH$_2$**-), 29.33 ppm (-**CH$_2$**-), 20.49 ppm (-**CH$_2$**-), and 14.06 (-**CH$_3$**) ppm.

2.5. Solid-state NMR measurements

Solid-state ^{13}C/^{15}N CP-MAS NMR spectra of polymorph I were obtained on a Bruker Avance III 400 MHz (B_0 = 9.4 T) NMR spectrometer operating at 100.61/40.56 MHz for ^{13}C/^{15}N, respectively, while high resolution solid-state ^{13}C/^{15}N CP-MAS NMR spectra of polymorph II were recorded on a Bruker Avance III 850 MHz (B_0 = 19.975 T) NMR spectrometer operating at 213.8/86.1 MHz for ^{13}C/^{15}N, respectively. NMR spectra were recorded using cross-polarisation (CP) from protons together with broadband decoupling using the spinal64 sequence [34] at the proton resonance to average out dipole-dipole ^{13}C-^{1}H/^{15}N-^{1}H interactions. The ^{13}C/^{15}N spectra were recorded under MAS conditions at spinning frequencies of 6-10 kHz; the proton $\pi/2$ pulse duration 2.7/2.5 μs (at 400 MHz) and 3.9/3.5 μs (at 850 MHz) μs; ^{1}H-^{13}C/^{1}H-^{15}N contact time 3.0/2.5 ms (at 400 MHz) 1.0/2.0 ms (at 850 MHz); the repetition time was 3.0 s. Isotropic chemical shifts were referenced to adamantane (38.48 ppm w.r.t TMS at 0.0 ppm) [35] in ^{13}C NMR and crystalline NH$_4$Cl (39.2 ppm w.r.t. NH$_3$ at 0.0 ppm) [36] in ^{15}N NMR.

Both non-centrosymmetric (polymorph I) and centrosymmetric (polymorph II) binuclear tris(di-*n*-butyldithiocarbamato)bismuth(III) complexes were characterised by ^{13}C and ^{15}N CP-MAS NMR (δ, ppm).

Polymorph I, $[Bi_2\{S_2CN(n\text{-}C_4H_9)_2\}_6]$:

^{13}C CP-MAS NMR (ppm) (see Fig. 2a) 206.1, 205.4, 202.3, 201.4, 201.1, 200.2 (1:1:1:1:1:1, -**S₂CN**=); 55.7, 55.5, 55.1, 54.7, 54.0, 53.7, 52.7 (2:1:1:3:2:2:1, =N**CH₂**-); 31.6, 30.9, 30.6, 29.6, 29.3, 29.2, 28.9, 28.7 (1:1:3:2:1:2:1:1, -**CH₂**-); 21.9, 21.5, 21.1, 20.4 (1:1:9:1, -**CH₂**-**CH₃**); 16.8, 15.9, 15.4, 15.0, 14.7, 14.1, 13.8 (1:1:1:3:3:1:2, -**CH₃**);

^{15}N CP-MAS NMR (ppm) (see Fig. 3a) 180.8, 180.2, 178.0, 174.4, 169.1 (2:1:1:1:1, =**N**-).

Polymorph II, $[Bi_2\{S_2CN(n\text{-}C_4H_9)_2\}_6]$:

^{13}C CP-MAS NMR (ppm) (see Fig. 2b) 204.7, 203.6, 199.9 (1:1:1, -**S₂CN**=); 56.6, 55.8, 54.9, 54.2, 53.6 (2:1:1:1:1, =N**CH₂**-); 30.8, 30.5, 29.6, 29.1, 28.8 (1:2:1:1:1, -**CH₂**-); 21.6, 21.3, 20.9, 20.8 (1:2:1:2, -**CH₂**-**CH₃**); 15.5, 15.4, 15.1, 14.2 (2:1:1:2, -**CH₃**).

^{15}N CP-MAS NMR (ppm) (see Fig. 3b) 177.3, 171.2, 167.7 (1:1:1)

2.6. X-ray diffraction (XRD) structure determination

The X-ray reflections of the single crystals of polymorphs I and II were collected on a Bruker APEX-II and Bruker Nonius Kappa CCD diffractometer, respectively, using Mo Kα (λ = 0.71073 Å) radiation. Data reduction was performed using Bruker SAINT software, while the intensities for absorption were corrected using SADABS. The structures were solved and refined using SHELS-2013 and SHELXL-2013, respectively, for non-H atoms [37,38]. The non-H atoms were refined with anisotropic displacement parameters. The H-atoms were positioned geometrically (methyl groups 0.96 Å and methylene groups 0.97 Å) and refined using riding models in which the isotropic thermal parameters of the H-atoms are proportional to those of the carbon atoms to which they are attached. In the case of II, the site

occupation factors of the butyl ligands were refined along with positional and displacement parameters. The final site occupancy factors for the six butyl groups were:

Bu(11): C11A-C12A-C13A-C14A [0.444(16)] and C11B-C12B-C13B-C14B [0.556(16)],

Bu(12): C15A-C16A-C17A-C18A [0.543(13)] and C15B-C16B-C17B-C18B [0.457(13)],

Bu(21): C21A-C22A-C23A-C24A [0.608(13)] and C21B-C22B-C23B-C24B [0.392(13)],

Bu(22): C25A-C26A-C27A-C28A [0.805(15)] and C25B-C26B-C27B-C28B [0.195(15)],

Bu(31): C31A-C32A-C33A-C34A [0.723(19)] and C31B-C32B-C33B-C34B [0.277(19)] and

Bu(32): C35A-C36A-C37A-C38A [0.713(17)] and C35B-C36B-C37B-C38B [0.287(17)].

Further information in the form of CIF has been deposited as depository CCDC 1458699 and 1494946 for forms I and II, respectively. A check of the final CIF file using PLATON did not show any missed symmetry. The data can be obtained free of charge via http://www.ccdc.cam.ac.uk or by contacting the Cambridge Crystallography Data Centre, 12 Union Road, Cambridge, UK.

2.7. Computational details of periodic calculation

Geometry optimisations were carried out at the DFT level of theory using the Perdew Burke Ernzerhof (PBE) functional [39] with a Tkatchenko-Scheffler (TS) dispersion correction [40], as implemented in the plane wave code CASTEP [31,41]. The structures were described as an infinite periodic solid using periodic boundary conditions. For NMR shielding constant calculations, the all-electron information was reconstructed using GIPAW [30] method as implemented in NMR CASTEP 7.0 code [30-32]. The geometry optimisations were performed using the ultra-soft pseudopotentials[32]. The total energy of the system was converged within 1E-7 eV. For geometry optimization, the Monkhorst-Pack k-point meshes with a grid of 0.03Å^{-1} for Brillouin zone sample with cut-off energy of 500 eV were chosen to achieve the total energy convergence of < 0.05 eV/atom. For NMR calculations, we have used a little higher energy cut-off (550 eV), which was tested to give sufficiently converged

NMR parameters (< 0.1 ppm). The integrals over the Brillouin zone were performed using a 2 x 2 x 1 (polymorph I) and 4 x 4 x 2 (polymorphs II and II^s) Monkhorst-Pack grid of k-points corresponding to less than 0.03 Å^{-1} separation between them in each reciprocal lattice directions.

Within the periodic boundary conditions, we have performed geometry optimisation of the crystal structures of I, II, and II^s either by relaxing positions of only hydrogens (H-opt) or all the atoms (full-opt) in the simulation cell. In both cases, the lattice parameters were kept fixed. The forces acting on atoms were converged below 0.01 eV/Å in geometry optimisation.

As was explained in section 2.6 of Material and Methods, because of the partial atom occupancy of some of the butyl carbons in polymorph II, the disordered dithiocarbamate ligands were considered as having two conformations (conformer-A and conformer-B, see Fig. 4b for labelling scheme). The geometry optimisation of crystal structure was performed by considering these two conformations separately. The calculated chemical shift is, therefore, a weighted average of the chemical shifts for the six disordered butyl ligands. The site occupancy factors (s.o.f.) of these ligands are also given in section 2.6.

For direct comparison of the GIPAW calculated ^{13}C shieldings with the experimentally measured isotropic chemical shift values the following expression was used,

$$\delta_{iso,calc} = \sigma_{ref} - \sigma_{iso} \tag{1}$$

where σ_{ref} = 170.9 ppm and 234.7 ppm for ^{13}C (TMS) and ^{15}N (NH$_3$), respectively [28].

3. Results and Discussion

3.1 Powder X-ray diffraction (PXRD)

The experimental PXRD patterns for the polymorphs I and II were compared with calculated PXRD patterns for the corresponding experimental X-ray structures (see Figs. 1a and 1b).

Although there are small discrepancies in the intensities and positions of certain peaks in the experimental *vs*. calculated PXRD patterns, here we only focus on the main features of resemblance between them. A qualitative comparison based on a visual assessment reveals a good matching between the experimental and calculated PXRD patterns for both the polymorphs, which ensures that the PXRD patterns of synthesised materials and hence the solid-state NMR spectra corresponds to their single crystal structures. It is known that an experimental PXRD pattern can be influenced, apart from the features of the instrumentation and method of data collection, by several factors related to the microstructural characteristics of the powder sample such as the size, shape and orientational distribution of the crystallites in the powder [42]. It is important that for a quantitative fitting of the experimental and the calculated peak profiles, a rigorous consideration of Rietveld refinement is needed [42,43].

3.2 Single crystal X-Ray diffraction

High quality single crystals of the polymorphs I and II were obtained and their structures determined as explained earlier (see section 2.6). The crystallographic data are given in Table 1. The ORTEP representation of the molecular structure of polymorph I is depicted in Fig. 4. Some selected interatomic distances and bond angles for polymorph I are given in Tables S1 and S2 in the ESI, respectively. The molecular structures of polymorphs II and II^s [29], along with the crystallographic labelling scheme, are depicted in Figs. 5a and S2 (see the ESI), respectively. In Tables S3 and S4 in the ESI, we have compared some selected bond distances and bond angles, respectively, for the polymorphs II with the corresponding bonds of II^s. The molecule of composition [Bi{S$_2$CN(n-C$_4$H$_9$)$_2$}$_3$] is the main structural unit of these binuclear compounds. There are four structurally inequivalent (isomeric) mononuclear molecules of bismuth di-n-butyldithiocarbamate in polymorph I and a single kind of [Bi{S$_2$CN(n-C$_4$H$_9$)$_2$}$_3$] in polymorph II. Therefore, in the former case, a combination of these

mononuclear species yields two isomeric non-centrosymmetric binuclear molecules of [$Bi_2\{S_2CN(n\text{-}C_4H_9)_2\}_6$] (polymorph I); whereas, there is a single kind of centrosymmetric binuclear molecule of the same composition [$Bi_2\{S_2CN(n\text{-}C_4H_9)_2\}_6$] in the latter case (polymorph II). The bismuth atoms form [BiS_6] chromophores of distorted pentagonal bipyramidal geometries, in which the lone pair of stereochemically active electrons originating from the central metal atom occupies one of the axial positions. Each bismuth atom in the considered molecules is coordinated in the *S,S'*-aniso-bidentate manner to three non-equivalent dithiocarbamate ligands: for all di-*n*-butyldithiocarbamate ligands, one of the Bi-S bonds is markedly stronger (polymorph I: 2.642(3)-2.798(3) Å) and (polymorph II: 2.582(2)-2.806(3) Å) than the other (polymorph I: 2.840(3)-3.110(3) Å) and (polymorph II: 2.790(3)-2.906(3)). The C-N bond lengths, which range from 1.312(14) to 1.370(13) Å, are shorter than the ideal C-N single bonds (1.47 Å) because of the double bond contribution in the dithiocarbamate ligands.

At the supramolecular level of polymorph I, isomeric non-centrosymmetric binuclear molecules of [$Bi_2\{S_2CN(n\text{-}C_4H_9)_2\}_6$] are formed by the pairs of relatively weak unsymmetrical secondary bonds between the mononuclear moieties: Bi(1)···S(7) (3.088 Å), Bi(2)···S(1) (3.039 Å) and Bi(3)···S(19) (3.141 Å), Bi(4)···S(18) (3.110 Å). For each dimer, the equatorial planes, where mononuclear molecules come close to each other, are mutually parallel. The combination of mononuclear [$Bi\{S_2CN(n\text{-}C_4H_9)_2\}_3$] molecules is purely based on structural selectivity. In the polymorph I, two inequivalent molecules come together because of the pairs of weak Bi···S interactions to form a non-centrosymmetric dimer unlike in polymorph II where a centrosymmetric dimer is formed because of the interaction of two equivalent molecular units with a Bi···S distance of 3.3898(10) Å (see Fig. 5b). The reported secondary Bi···S distance in the polymorph II^s was 3.3629(34) Å [29].

The crystal structure of II has been solved and refined in the setting $P2_1/n$ of space group 14 rather than in $P2_1/c$ as reported by Sun *et al.* [29]. This gives the beta angle closer to 90°, which provides for more accurate computations, since the rounding errors are smaller. The unit cell parameters are as follows:

Polymorph II[s] [29]: $a = 16.802(9)$ Å, $b = 10.256(6)$ Å, $c = 25.083(10)$ Å, $\beta = 121.77(3)$°;

Polymorph II: $a = 16.932(4)$ Å, $b = 10.366(2)$ Å, $c = 21.817(4)$ Å, $\beta = 99.44(3)$°. Apart from that the polymorph II[s] does not display any conformational disorders [29]. However, in our case, it was found that all six butyl groups of II were disordered, because the butyl chains of all three dithiocarbamate ligands could adopt several different conformations. In some cases, there were even more possibilities of minor site occupancy factors, but we have only taken the two most common conformations (referred to as conformer-A and conformer-B in the following sections) (see Fig. 5a). The site occupation factors of the butyl groups of our structure are given in section 2.6 of Materials and Methods. The heavy atom root-mean-square deviation (RMSD) between the two conformers is 1.3 Å.

3.3 Solid-state ^{13}C and ^{15}N CP-MAS NMR spectra

In the ^{13}C NMR spectrum (solution in $CDCl_3$) of tris(di-*n*-butyldithiocarbamato)bismuth(III) one observes resonances for each inequivalent carbon atom in the molecule i.e., single resonance lines for $–S_2CN$, $-NCH_2-$, $-CH_2-$, $-CH_2-$, and $-CH_3$ groups (see Fig. S1b in ESI). On the other hand, Fig. 2a shows a solid-state ^{13}C CP-MAS NMR spectrum of the polycrystalline sample of polymorph I, depicting multiple resonance lines representing inequivalent carbons. The signal enhancement of a CP-MAS experiment depends largely on the proton spin-lattice relaxation time ($T_1{}^H$) and the competition between T_{CP} and $T_1\rho^H$ during CP transfer, where T_{CP} and $T_1\rho^H$ represents CP time (contact pulse width) and proton spin-lattice relaxation time during CP. Since these relaxation parameters are usually different for atoms in chemically

inequivalent sites, the observed signal enhancements may vary significantly. In our case, to quantify the number of sites of each kind the peaks corresponding to the atoms in the same position in the molecule are compared. The most informative region of the dithiocarbamate ligands i.e., $-S_2CN-$ carbons, resulted in six well resolved ^{13}C resonance signals with chemical shifts over a range of 200.2-206.1 ppm with relative integral intensities of 1:1:1:1:1:1 indicating the presence of at least six structurally inequivalent n-butyldithiocarbamate ligands in the unit cell. However, we expect twelve resonance lines for dithiocarbamate groups, as there are twelve inequivalent sites revealed from the X-ray diffraction structure but there is an insufficient resolution in the NMR spectrum for this observation. Additionally, in the ^{13}C CP-MAS spectrum of the polymorph I, one observes ^{13}C resonances corresponding to twelve carbons each for four alkyl carbons of the butyl chains. On the other hand, five resonance signals with chemical shifts over a range of 169.1-180.8 ppm with an integrated intensity ratio of 2:1:1:1:1 were observed in the ^{15}N CP-MAS NMR spectrum (see Fig. 3a), again suggesting the presence of at least six inequivalent nitrogen sites in the dithiocarbamate ligands of the complex.

On the contrary, both ^{13}C and ^{15}N CP-MAS spectra for the centrosymmetric binuclear $[Bi_2\{S_2CN(-n-C_4H_9)_2\}_6]$ complex (polymorph II) are more simple: both spectra show only three resonance signals for dithiocarbamate groups with relative integral intensities of 1:1:1 for both ^{13}C and ^{15}N sites, both indicating the presence of only three inequivalent di-n-butyldithiocarbamate ligands (see Figs. 2b and 3b). The solid-state NMR spectral assignments for selected carbon and nitrogen sites are suggested in Tables 6 and 7, respectively.

Overall, the ^{13}C and ^{15}N CP-MAS NMR data of polymorph I agree well with single crystal XRD data indicating that the system under consideration contains a minimum of six structurally inequivalent dithiocarbamate groups. Similarly, the single crystal XRD data for

the polymorph II show the presence of a centrosymmetric binuclear molecule of [Bi$_2$\{(S$_2$CN(n-C$_4$H$_9$)$_2$)$_6$\}], which is in accord with the ^{13}C and ^{15}N chemical shift data suggesting at least three structurally inequivalent dithiocarbamate groups in this conformer.

3.4 Geometry optimisation and NMR calculations

The experimental chemical shifts for both polymorphs I and II are compared with those calculated from DFT/GIPAW approach (see Tables 6 and 7). The calculated ^{13}C/^{15}N nuclear shielding values for some selected atoms of polymorphs I, II and II^s are listed in Tables S1 and S2 (see the ESI), respectively. In CASTEP, the ^{13}C and ^{15}N NMR chemical shift calculations were performed at both the "H-opt" and "full-opt" geometry of polymorphs I, II and II^s. The strong forces on the atoms indicate that the structural model derived from diffraction requires optimisation of the atomic coordinates. The forces on non-proton atoms of "H-opt" structures were fairly large (> 2 eV/Å) while in the "full-opt" structures the forces on all atoms were reduced below 0.01 eV/Å. The CASTEP calculated bond lengths and bond angles are compared with the actual (experimental) values in Tables S1-S4 in the ESI. The heavy atom RMSD between the "H-opt" and "full-opt" structures of polymorph I was 0.07 Å. In case of polymorph I, the calculated bond parameters are very close to the experimental values. However, the NMR chemicals shifts are known to be very sensitive even to small variations in the bond parameters. Therefore, the geometry optimisation of the X-ray structures will have a large and direct effect on the calculated chemical shifts. Based on the geometrical close resemblance and the calculated NMR chemical shift results of the "full-opt" structure, we have grouped the dithiocarbamate ligands as either 'terminal' or 'bridged' (see Tables 6 and 7). In polymorph I, the experimental NMR spectral assignments of different dithiocarbamate sites were made based on the observations that both the bonding parameters and the calculated NMR chemical shifts show a close resemblance between Bi1 and Bi4 as

well as Bi2 and Bi3 molecular units. Although both "H-opt" and "full-opt" structures produce almost similar ^{13}C chemical shifts, the ^{15}N chemicals shifts of "H-opt" structure was rather random (see Tables 2) indicating that the latter are more sensitive to the subtle structural changes. Therefore, it is not possible to show any meaningful correlation between the calculated and the experimental ^{15}N NMR chemical shifts for different dithiocarbamate sites based on the "H-opt" structure. Moreover, it does not allow us to group them as 'bridged' or 'terminal' dithiocarbamate ligands. As can be seen from Tables 2, for the "full-opt" structure, the ^{13}C chemical shifts for the bridged dithiocarbamate carbons appear more deshielded than the terminal dithiocarbamate carbons. In the ^{13}C CP-MAS NMR spectra of polymorph I (Figure 3a), the higher (more deshielded) chemical shifts at 206.1 and 205.4 ppm can be attributed to the bridging dithiocarbamate carbons, while the terminal ligands have lower (more shielded) chemical shifts between 202.3 – 200.2 ppm (see Tables 2). On the contrary, the ^{15}N CP-MAS NMR resonance lines for nitrogen sites in the bridging dithiocarbamate ligands are more shielded (169.1 and 174.3 ppm) as compared to the terminal ligands (178.0-180.8 ppm). The experimental chemical shift ranges for $^{13}C/^{15}N$ dithiocarbamate sites in polymorph I are 6.1/11.7 ppm while the calculated chemical shift ranges are 6.9/18.5 ppm.

There is clearly a good agreement between the experimental and theoretical ^{13}C and ^{15}N data as confirmed by the linear regression plots (with slopes and R^2 very close to unity) for the experimental *vs*. calculated (GIPAW) chemical shifts for the "full-opt" structure of the polymorph I (Figs. 6a and 6b, respectively). A similar ^{13}C correlation plot corresponding to the "H-opt" structure is shown in Fig. S3a in the ESI. The root-mean-square deviation (RMSD) between the experimental and the calculated $^{13}C/^{15}N$ chemical shifts for the "full-opt" and the "H-opt" structures are also compared in Tables 2. The lower RMSDs for the "full-opt" structure, again, indicate a better correspondence with the experimental values.

The sources of discrepancies in the calculated $^{13}C/^{15}N$ chemical shifts observed for "H-opt" structure can be any or all of the following: (i) The reported uncertainties in atomic positions from diffraction measurements can lead to significant variations in computed chemical shifts; (ii) The DFT calculations were done at zero K (without zero-point vibrations) whereas the experimental determinations are performed under very different circumstances (100.0 K for structure determination and at room temperature (298 K) for all NMR measurements) [45]. The improved NMR results in case of the "full-opt" structure is most probably because of the converged forces on atoms, which were still rather large in the X-ray structure indicating a non-equilibrium state of the system [44,45]. The close-to equilibrium structure is a prerequisite to get reasonable assignments of NMR spectra, as without vibrational averaging of modelled parameters it is the best approximation of the real (temperature) averaged structure corresponding to the experimentally observed NMR chemical shifts.

In Tables 3, we have compared the experimental NMR chemical shifts with those calculated for the "H-opt" and "full-opt" structures of polymorph II. As explained before, the geometry optimisation of polymorph II was performed by considering the disordered pairs for each of the dithiocarbamate ligands separately. Therefore, in all cases, the chemical shifts for polymorph II were calculated as the average over conformationally disordered ligands. Although the calculated ^{13}C and ^{15}N chemical shifts for the "H-opt" structure qualitatively represents the experimental spectral pattern, the dithiocarbamate ligands show deviations in terms of the chemical shift range as well as the relative chemical shift difference between the inequivalent sites. For example, the experimental $^{13}C/^{15}N$ chemical shift ranges for–S_2CN sites are relatively smaller (4.7/9.6 ppm) compared to the calculated ones (10.4/11.4 ppm). Furthermore, the relative difference between the calculated chemical shift for two of the dithiocarbamate carbons viz., C3 and C2, is much larger (8.7 ppm) than the experimentally observed difference between them (1.0 ppm). Similarly, the calculated and experimental ^{15}N

chemical shift difference between N2 and N3 are 10.6 and 3.5 ppm, respectively. On the other hand, as indicated from the lower RMSD values (see Tables 3), the calculated $^{13}C/^{15}N$ chemical shifts for the "full-opt" structure of polymorph II showed in a much better agreement with the experimental values than for the "H-opt" structure. Also, in terms of both the NMR chemical shift range and the relative difference between the resonance lines for inequivalent ligand sites, the calculated chemical shifts for the "full-opt" structure better represents the observed chemical shifts. The plots of experimental vs. calculated ^{13}C chemical shifts for the "full-opt" structure of II displays an excellent linear correlation (R^2 close to unity) (see Fig. 6c). The ^{13}C experimental *vs.* calculated correlation plot for the "H-opt" structure of II is depicted in Figs. S3b (see the ESI).

As can be seen from Tables S3 and S4 in the ESI, there is a significant difference in some of the experimental bond parameters between the crystal structures of II and II^s. Many of the bond distances are not equal within the experimental error limits, especially, for the C-N, alkyl chain N-C and C-C bonds. For example, the reported C-N bond lengths for II^s (1.31(1)-1.33(2) Å) are shorter compared to our structure II (1.341(12)-1.354(12) Å) while the DFT calculated bond distances vary between 1.349-1.356 Å, which is much closer to our experimental results. A much shorter C-C bond lengths have been reported for II^s, e.g. C21-C22 is 1.38(3) Å while the corresponding C-C bond distances in our structure is 1.556(10)-1.562(10) Å, which is again very close to the DFT calculated bond distances. Many such differences were also observed in the alkyl N-C/C-C bond lengths and N-C-C/C-C-C bond angles of other two dithiocarbamate ligands (not shown in Table 5). The heavy atom RMSD between the dimers of II and II^s is 2.1 Å (see Fig. S4 in the ESI). Also, slightly longer Bi···S bond length of 3.3898(10) Å for II (see Fig. 5b) *vs.* 3.3629(34) Å for II^s [29] and Bi-Bi distance of 4.850 Å for II (see Fig. 5b) vs. 4.807 Å for II^s [29] indicate a slight variation in the intermolecular interaction between the mononuclear molecules at the supramolecular level. In

addition, as mentioned in section 2.6, the three dithiocarbamate ligands for polymorph II have conformational disorders, while the reported crystal structure for II^s does not. The DFT calculated bond parameters for the "full-opt" structure of II^s are very close, but not identical, to those calculated for polymorph II. In Fig. S5 (see the ESI), we have overlaid the "full-opt" mononuclear molecular units for the polymorph II^s and the two conformers of polymorph II. The "full-opt" structure of II^s follows conformer-A of polymorph II with an RMSD of 0.06 Å (see Tables S3 and S4 in the ESI).

In order to understand how the experimentally observed differences in the bond parameters between the crystal structures for the polymorphs II and II^s (see Tables S3 and S4 in the ESI) affect their calculated NMR chemical shifts, we have compared the GIPAW calculated chemical shifts for the "H-opt" structures of both II and II^s (see Tables 3). Although the calculated ^{13}C chemical shifts of butyl carbons (averaged for different dithiocarbamate ligands) for the "H-opt" structure of II^s are somewhat closer to those calculated for II, both ^{13}C and ^{15}N chemical shifts of dithiocarbamate sites show much larger deviations. On the other hand, the calculated chemical shifts for the "full-opt" structures of II^s and II are much closer to each other (see Tables 3). In addition, we have also calculated the RMSD between the experimental ^{13}C/^{15}N chemical shifts that corresponds to polymorph II and those calculated for II^s (see Tables 3). It is observed that the RMSD decreases from 6.1/12.7 (H-opt) to 0.8/2.5 (full-opt) indicating that the "full-opt" structure for II^s, having the bond parameters similar to that of the "full-opt" structure for II, provides a better comparison than the "H-opt" structure for II^s.

4. Conclusions

Two crystalline polymorphs of tris(di-*n*-butyldithiocarbamato)bismuth(III) complex, referred to as I and II, were synthesised and characterised by using a combination of experimental solid-state ^{13}C/^{15}N CP-MAS NMR, powder and single crystal X-ray diffraction methods, and

periodic DFT/GIPAW computations. The single crystal structure of polymorph I, having two isomeric non-centrosymmetric binuclear molecules of $[Bi_2\{S_2CN(n\text{-}C_4H_9)_2\}_6]$ at the supramolecular level, was described in the triclinic system of $P\bar{1}$ space group. On the other hand, the crystal structure of polymorph II comprising one kind of centrosymmetric molecules of $[Bi_2\{S_2CN(n\text{-}C_4H_9)_2\}_6]$ was solved in the monoclinic system of $P2_1/n$ space group, which is similar to, but not identical with, a previously reported crystal structure of the title complex by Sun *et al*. [29]. It was also found that polymorph I was readily convertible to polymorph II by changing the solvent system from acetonitrile to dichloromethane and *vice versa* during the recrystallisation. We have suggested the crystallographic assignments for the ^{13}C and ^{15}N resonance lines in NMR spectra of both polymorphs by comparing them with the GIPAW calculated chemical shifts. Because of large forces on atoms of the experimental XRD structures, the best correspondence with the experimental NMR chemical shifts were obtained when the atomic positions of all atoms in the single crystal structures of both polymorphs were optimised.

Acknowledgements

Appendix A. Supplementary data

CCDC 1458699 and 1494946 contains the supplementary crystallographic data for polymorphs I (non-centrosymmetric molecules of [$Bi_2\{(S_2CN(n\text{-}C_4H_9)_2\}_6$] and II (centrosymmetric molecules of [$Bi_2\{(S_2CN(n\text{-}C_4H_9)_2\}_6$]. These data can be obtained free of charge via http://www.ccdc.cam.ac.uk/conts/retrieving.html. or from the Cambridge Crystallographic Data Centre, 12 Union Road, Cambridge CB2 1EZ, UK; fax: (+44) 1223-336-033; or e-mail: deposit@ccdc.cam.ac.uk.

References

[1] S. Patai, The chemistry of organic arsenic, antimony and bismuth compounds, John Wiley and Sons, Chichester, 1994.

[2] H. Li, H. Sun, Curr. Opin. Chem. Biol., 16 (2012) 74-83.

[3] G.G. Briand, N. Burford, Chem. Rev., 99 (1999) 2601-2658.

[4] M.D. Regulacio, N. Tomson, S.L. Stoll, Chem. Mater., 17 (2005) 3114-3121.

[5] O.C. Monteiro, H.I.S. Nogueira, T. Trindade, M. Motevalli, Chem. Mater., 13 (2001) 2103-2111.

[6] S.A. Afrillya, Y. Mulyasih, I. Hastiawan, In Proceeding of the International Seminar on Chemistry, Jatinangor, (2008) 186-190.

[7] F.U. Shah, S. Glavatskih, O.N. Antzutkin, Tribol. Lett., 45 (2012) 67-78.

[8] J. Sedlacek, L.M. Martins, P. Danek, A.J. Pombeiro, B. Cvek, J. Appl. Biomed., 12 (2014) 301-308.

[9] H. Li, C.S. Lai, J. Wu, P.C. Ho, D. de Vos, E.R.T. Tiekink, J. Inorg. Biochem., 101 (2007) 809-816.

[10] G. Hogarth, Mini-Rev. Med. Chem., 12 (2012) 1202-1215.

[11] R.A. Ludwig, G.D. Thorn, Adv. Pest Control Res., 3 (1960) 219-252.

[12] G.D. Thorn, R.A. Ludwig, The dithiocarbamates and related compounds, Elsevier, Amsterdam, 1962, pp. 224-260.

[13] G. Hogarth, Transition metal dithiocarbamates: 1978–2003, Prog. Inorg. Chem., 53 (2005) 71-561.

[14] A.V. Ivanov, I.V. Egorova, M.A. Ivanov, O.N. Antzutkin, R.S. Tsvykh, Dokl. Phys. Chem., 454 (2014) 16-20.

[15] S.S. Garje, V.K. Jain, Coord. Chem. Rev., 236 (2003) 35-56.

[16] C.S. Lai, E.R.T. Tiekink, Z. Kristallogr., 222 (2007) 532-538.

[17] H.G. Brittain, Polymorphism in pharmaceutical solids, second ed., New York, CRC Press 2016.

[18] R.K. Harris, J. Pharm. Pharmacol., 59 (2007) 225-239.

[19] A.V. Ivanov, O.N. Antzutkin, Top. Curr. Chem., 246 (2005) 271-337.

[20] R. Purohit, P. Venugopalan, Reson., 14 (2009) 882-893.

[21] S.E. Ashbrook, D. McKay, Chem. Comm., 52 (2016) 7186-7204.

[22] R.K. Harris, R.E. Wasylishen, M.J. Duer, NMR Crystallography, Wiley, New York, 2009.

[23] S. Sneddon, D.M. Dawson, C.J. Pickard, S.E. Ashbrook, Phys. Chem. Chem. Phys., 16 (2014) 2660-2673.

[24] C. Martineau, Solid State Nucl. Magn. Reson., 63 (2014) 1-12.

[25] C. Martineau, A. Cadiau, B. Bouchevreau, J. Senker, F. Taulelle, K. Adil, Dalton Trans., 41 (2012) 6232-6241.

[26] R.K. Harris, Solid State Sci., 6 (2004) 1025-1037.

[27] V. Gowda, B. Sarma, S. Öberg, V.-V. Telkki, A.-C. Larsson, P. Lantto, O.N. Antzutkin, Eur. J. Inorg. Chem., 20 (2016) 3278-3291.

[28] V. Gowda, R.S. Laitinen, V.-V. Telkki, A.-C. Larsson, O.N. Antzutkin, P. Lantto, Dalton Trans. 45 (2016) 19473-19484.

[29] R.Z. Sun, Y.S. Guo, W.M. Liu, S.Y. Chen, Y.Q. Feng, Chinese J. Struct. Chem., 31 (2012) 655-660.

[30] C.J. Pickard, F. Mauri, Phys. Rev. B., 63 (2001) 245101.

[31] S.J. Clark, M.D. Segall, C.J. Pickard, P.J. Hasnip, M.I. Probert, K. Refson, M.C. Payne, Z. Kristallogr., 220 (2005) 567-570.

[32] J.R. Yates, C.J. Pickard, F. Mauri, Phys. Rev. B, 76 (2007) 024401.

[33] C.F. Macrae, P.R. Edgington, P. McCabe, E. Pidcock, G.P. Shields, R. Taylor, M. Towler, J. van de Streek, J. Appl.Crystallogr., 39 (2006) 453-457.

[34] B. Fung, A. Khitrin, K. Ermolaev, J. Magn. Reson., 142 (2000) 97-101.

[35] C.R. Morcombe, K.W. Zilm, J. Magn. Reson., 162 (2003) 479-486.

[36] P. Bertani, J. Raya, B. Bechinger, Solid State Nucl. Magn. Reson., 61 (2014) 15-18.

[37] G.M. Sheldrick, Acta Crystallogr. Sect. A, 46 (1990) 467-473.

[38] G.M. Sheldrick, Acta Crystallogr. Sect. A, 64 (2007) 112-122.

[39] Y. Zhang, W. Yang, Phys. Rev. Lett., 80 (1998) 890.

[40] A. Tkatchenko, M. Scheffler, Phys. Rev. Lett., 102 (2009) 073005.

[41] M.D. Segall, P.J. Lindan, M.A. Probert, C.J. Pickard, P.J. Hasnip, S.J. Clark, M.C. Payne, J. Phys. Condens. Matter., 14 (2002) 2717-2744.

[42] I.Y. Bagryanskaya, Y.V. Gatilov, J. Struct. Chem., 24 (1983) 150-151.

[43] D.W Bruce, D. O'Hare, R.I. Walton, Structure from Diffraction Methods: Inorganic Materials Series, John Wiley and Sons, New York, 2014.

[44] K. Rissanen, Advanced X-ray crystallography, Springer, Heidelberg, 2012.

[45] R.K. Harris, P. Hodgkinson, C.J. Pickard, J.R. Yates, V. Zorin, Magn. Reson. Chem., 45 (2007) S174-S186.

Table 1. X-ray diffraction crystallographic data for polymorphs I and II.

Crystal Data	I	II
Empirical formula	$C_{27}H_{54}N_3S_6Bi$	$C_{27}H_{54}N_3S_6Bi$
Formula wt.	822.07	822.07
Crystal system	Triclinic	Monoclinic
T [K]	150	298 (2)
a [Å]	13.7919(3)	16.932(3)
b [Å]	16.7642(5)	10.366(2)
c [Å]	31.3282(7)	21.817(4)
α [°]	95.316(2)	90.0
β [°]	92.6420(10)	99.44(3)
γ [°]	94.0720(10)	90.0
Volume [Å³]	7183.9(3)	3777.3(14)
Space group	$P\bar{1}$	$P2_1/n$
Z	8	4
D_{calc} [g cm⁻³]	1.520	1.446
μ/mm⁻¹	5.278	5.019
Reflns. collected	104145	23705
Unique reflns.	28205	6644
Observed reflns.	17957	4396
R_1 [I>2σ(I)], wR_2	0.0568, 0.1369	0.0520, 0.0683
Instrument	Bruker APEX-II CCD	Bruker Nonius Kappa CCD

Tables 2. Experimental and theoretical (GIPAW/PBE) ^{13}C and ^{15}N chemical shifts of polymorph I.

Sites	Labels [a]	H-opt [b]	Full-opt [b]	Expt.
^{13}C Chemical shifts				
-S$_2$**C**-N	C1, C82	205.4	207.5	206.1
(bridged)	C28, C73	203.6	205.3	205.4
-S$_2$**C**-N	C19, C100	204.1	203.7	202.3
(terminal)	C46, C55	201.8	202.8	201.4
	C37, C64	201.7	202.2	201.1
	C10, C91	198.2	200.6	200.2
-N-**CH$_2$**-	Avg.	56.0	54.8	54.5
-**CH$_2$**-CH$_2$-	Avg.	28.6	27.9	29.9
-**CH$_2$**-CH$_3$	Avg.	19.6	20.1	21.2
-**CH$_3$**	Avg.	12.5	12.8	15.1
RMSD [c]		1.6	1.3	
^{15}N Chemical shifts				
-S$_2$C-**N**-	N2, N11	180.8	186.6	180.8
(terminal)	N3, N12	183.4	183.8	180.8
	N5, N8	175.0	182.1	180.2
	N6, N7	169.9	180.5	178.0
-S$_2$C-**N**-	N1, N10	183.0	173.9	174.4
(bridged)	N4, N9	184.8	168.1	169.1
RMSD [c]		8.4	3.0	

[a] For atom labelling scheme, see Fig. 4

[b] The stated chemical shifts are averages of the calculated values for the two sites. For isotropic shiedings values of each atoms, see Table S5 in the ESI.

[c] RMSD: Root-mean-square deviation between the experimental and calculated chemical shifts.

Ta bles 3. Experimental and theoretical (CASTEP/PBE) ^{13}C and ^{15}N chemical shifts for the polymorphs II and II^s.

Sites	Labels	H-opt[a]	Full-opt[a]	H-opt[b]	Full-opt[b]	Expt.[b]
^{13}C Chemical shifts						
-S$_2$**C**-N	C3	196.1	204.3	207.1	205.6	204.7
(Terminal)	C2	193.1	203.2	198.4	205.0	203.7
-S$_2$**C**-N	C1	191.4	199.9	196.7	201.3	200.0
(Bridged)						
-N-CH$_2$-	Avg.	55.7	55.7	57.7	56.7	55.0
-CH$_2$-CH$_2$-	Avg.	28.1	28.1	33.2	28.6	29.5
-CH$_2$-CH$_3$	Avg.	20.4	20.4	21.8	20.0	21.2
-CH$_3$	Avg.	14.4	14.4	15.3	14.1	15.1
RMSD[c]		6.1	0.8	3.1	1.2	-
^{15}N Chemical shifts						
-S$_2$**C**-N	N1	195.4	176.9	177.3	177.7	177.3
(Bridged)						
-S$_2$**C**-N	N3	172.6	175.0	170.1	175.8	171.2
(Terminal)	N2	157.3	169.8	163.5	169.9	167.7
RMSD[c]		12.7	2.5	3.3	2.9	-

[a] Polymorph II^s (Atom labelling scheme: C3=C1, C2=C10, C1=C19, N1=N3, N2=N2, and N3=N1, see Fig. 5a and S3 in the ESI)

[b] Polymorph II (For atom labelling scheme, see Fig. 5a)

[c] RMSD: Root-mean-square deviation between the experimental and calculated chemical shifts.

(a)

(b)
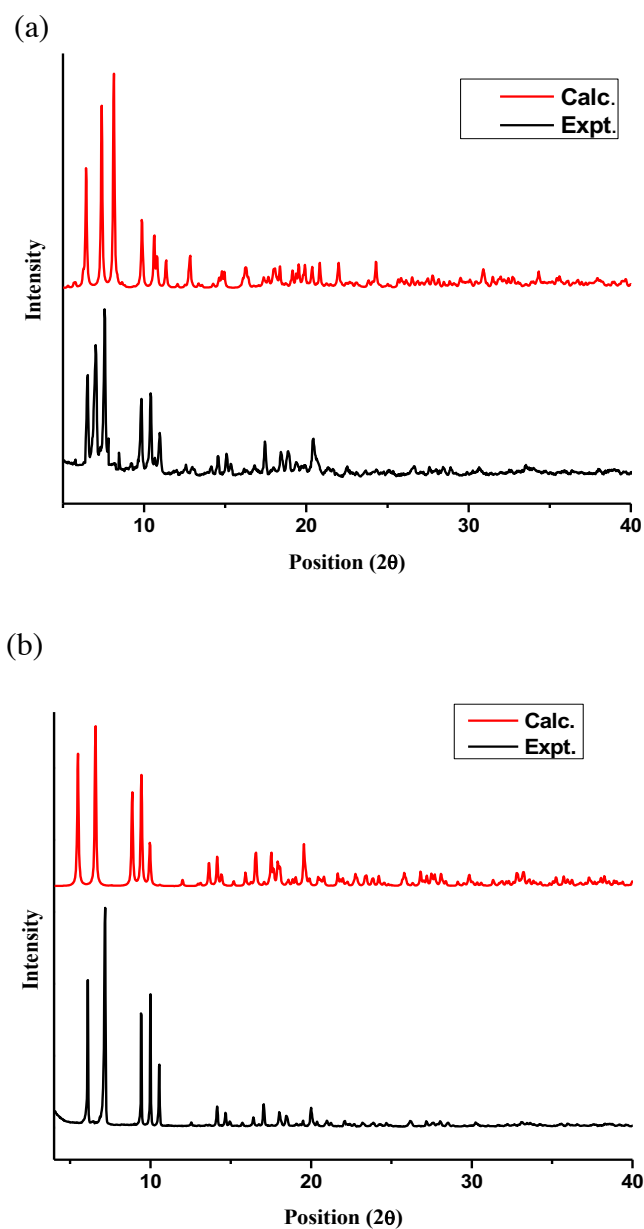
Fig. 1 Experimental and theoretically calculated powder X-ray diffraction (PXRD) patterns of polymorph I (**a**) and polymorph II (**b**).

(a)

(b)
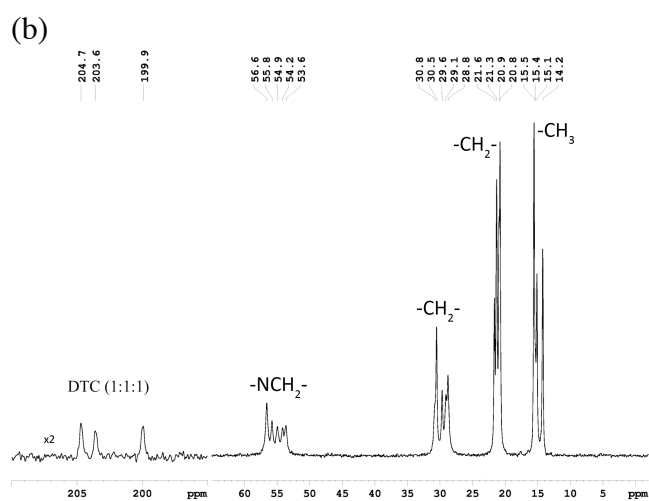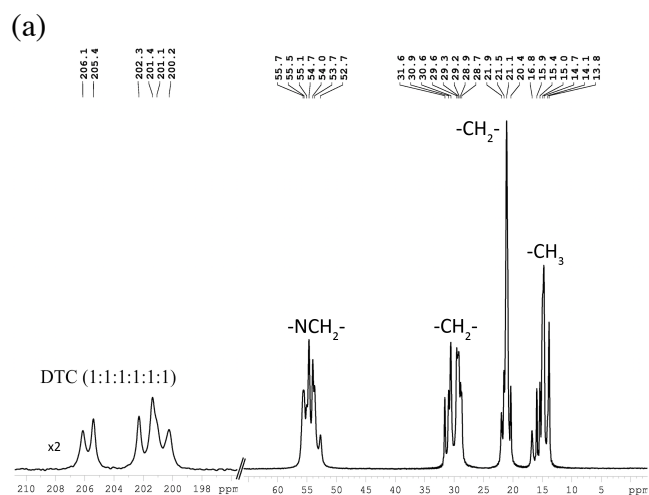
Fig. 2 ^{13}C CP-MAS spectra for polymorphs (**a**) for I (100.6 MHz) and (**b**) for II (213.8 MHz). The intensity of the dithiocarbamate carbons displayed along the y-axis has been doubled for clarity.

(a)

(b)
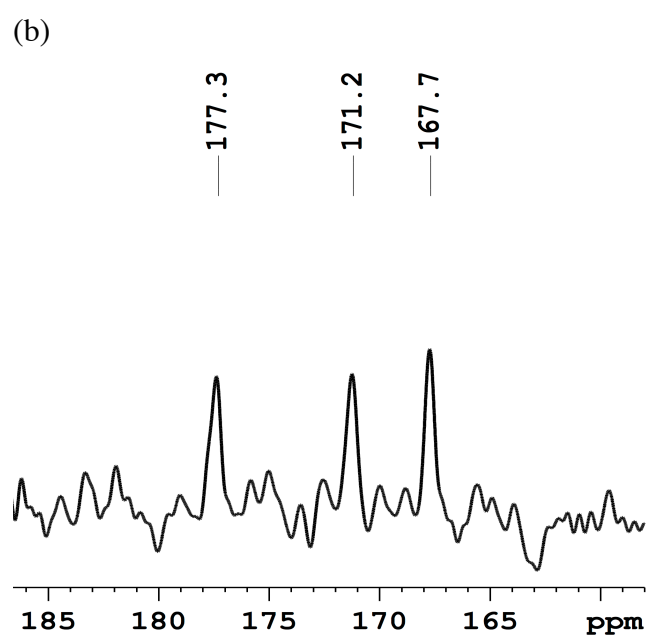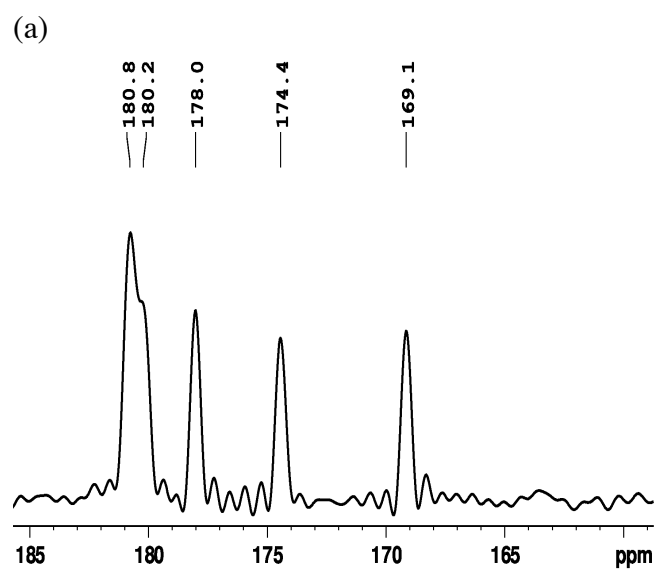
Fig. 3 ^{15}N CP-MAS spectra for polymorph I (40.6 MHz) (**a**) and polymorph II (86.1 MHz) (**b**).
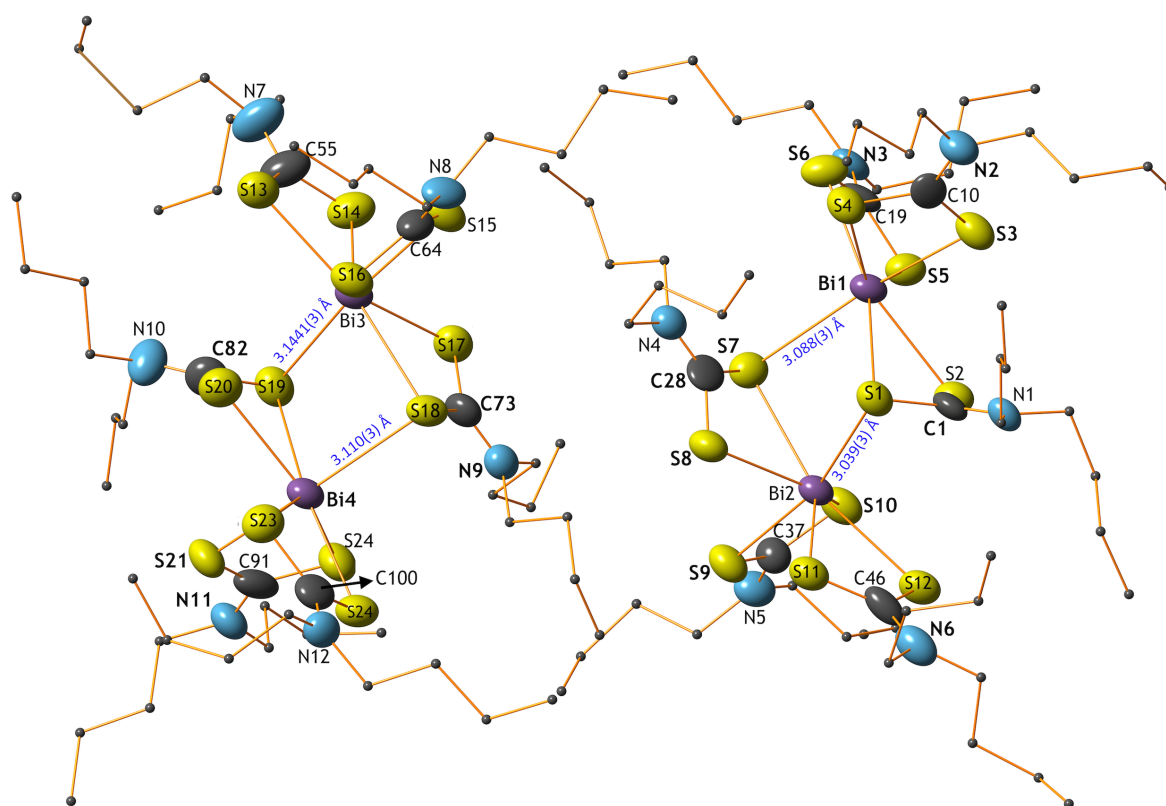
Fig. 4 Molecular structures of two non-centrosymmetric dimers of polymorph I, showing atom labelling scheme and thermal ellipsoids at the 50% probability level. For clarity, the alkyl chain carbon atoms have been drawn as ball-and-stick models while the H-atoms are omitted.

(**a**)
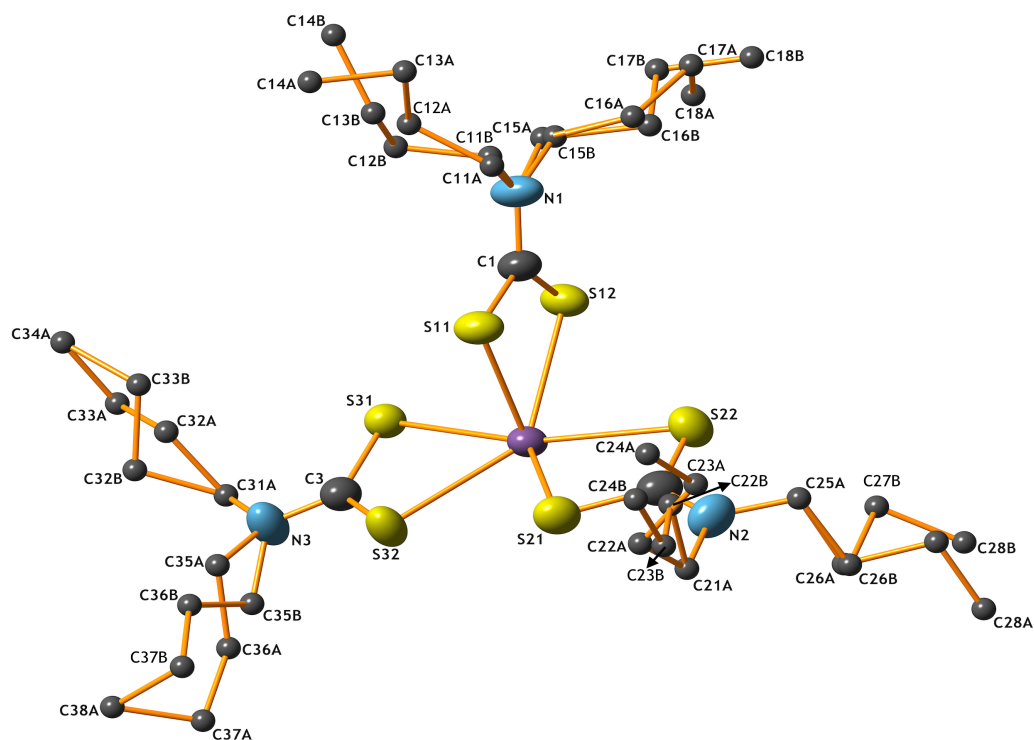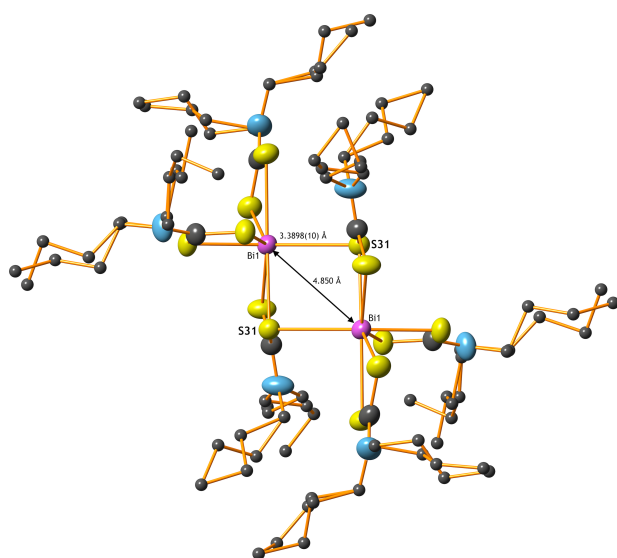
Fig. 5 (a) The molecular structure and atomic labelling scheme for polymorph II, showing displacement ellipsoids at the 50% probability level for non-alkyl chain atoms. The coordinates for atoms such as C21A, C25A, C31A and C34A are as same as their respective counterparts C21B, C25B, C31B and C34B, hence, the later atoms are not displayed. **(b)** The centrosymmetric binuclear molecules of $[Bi_2\{S_2CN(n\text{-}C_4H_9)_2\}_6]$ for polymorph II. For clarity, the alkyl chain carbon atoms have been drawn as ball-and-stick models while the H-atoms are omitted.
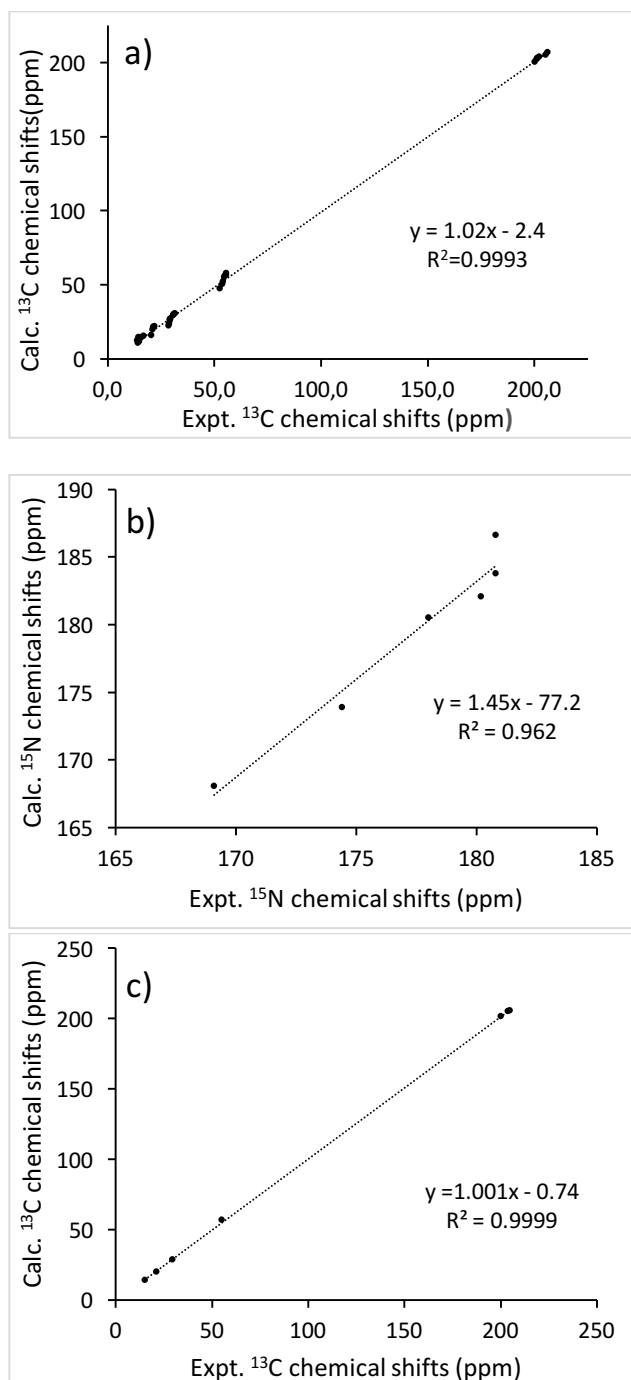
Fig. 6 Linear regression plots of calculated (Calc.) *vs*. experimental (Expt.) chemical shifts for full-opt structures: (**a**) polymorph I (^{13}C); (**b**) polymorph I (^{15}N); and (**c**) polymorph II (^{13}C). The shieldings for ^{13}C and ^{15}N were converted to chemical shifts using a reference value of 170.9 ppm and 234.7 ppm, respectively.

Electronic Supplementary Information (ESI) to the article

Structural Insights into the Polymorphism of Bismuth(III) Di-*n*-butyldithiocarbamate by X-Ray Diffraction, Solid-State (^{13}C/^{15}N) CP-MAS NMR, and DFT Calculations

Vasantha Gowda, Bipul Sarma, Risto S. Latinen, Anna-Carin Larsson, Alexander V. Ivanov,

Dinu Iuga, Perttu Lantto and Oleg N. Antzutkin

Table S1. Some selected experimental (Expt.) and CASTEP calculated (Calc.) bond lengths (Å) for polymorph I[a]

Bond angle	Expt.	Calc.	Bond angle	Expt.	Calc.
	Bi1			Bi4	
Bi1-S1	3.077(3)	3.0537	Bi4-S19	3.019(3)	2.9935
Bi1-S2	2.840(3)	2.8597	Bi4-S20	2.860(3)	2.9048
Bi1-S3	2.642(3)	2.6781	Bi4-S21	2.630(3)	2.6830
Bi1-S4	2.905(3)	2.8815	Bi4-S22	2.920(3)	2.8721
Bi1-S5	2.738(3)	2.7537	Bi4-S23	2.719(3)	2.7557
Bi1-S6	2.787(3)	2.7782	Bi4-S24	2.809(3)	2.7847
Bi1-S7	3.088(3)	2.9965	Bi4-S18	3.110(3)	2.9778
C1-N1	1.325(13)	1.3436	C82-N10	1.312(14)	1.3440
C10-N2	1.335(12)	1.3508	C91-N11	1.330(13)	1.3514
C19-N3	1.346(13)	1.3482	C100-N12	1.351(14)	1.3480
S1-C1	1.721(11)	1.7236	S19-C82	1.742(12)	1.7262
S2-C1	1.748(11)	1.7314	S20-C82	1.761(12)	1.7285
S3-C10	1.742(11)	1.7339	S21-C91	1.746(13)	1.7333
S4-C10	1.703(11)	1.7100	S22-C91	1.711(12)	1.7108
S5-C19	1.728(11)	1.7247	S23-C100	1.735(11)	1.7224
S6-C19	1.729(11)	1.7237	S24-C100	1.726(12)	1.7253
	Bi2			Bi3	
Bi2-S9	2.691(3)	2.7196	Bi3-S15	2.655(3)	2.6999
Bi2-S10	2.932(3)	2.9030	Bi3-S16	2.918(3)	2.8999
Bi2-S11	2.782(3)	2.8070	Bi3-S14	2.761(3)	2.7849
Bi2-S12	2.893(3)	2.8604	Bi3-S13	2.868(3)	2.8436
Bi2-S7	2.952(3)	2.9431	Bi3-S18	2.946(3)	2.9405
Bi2-S8	2.779(3)	2.8086	Bi3-S17	2.798(3)	2.8336
Bi2-S1	3.039(3)	2.9813	Bi3-S19	3.141(3)	3.0404
C28-N4	1.324(13)	1.3500	C55-N7	1.316(14)	1.3574
C37-N5	1.347(12)	1.3551	C64-N8	1.325(12)	1.3543
C46-N6	1.361(14)	1.3559	C73-N9	1.370(13)	1.3477
S7-C28	1.746(12)	1.7401	S13-C55	1.723(13)	1.7154
S8-C28	1.739(11)	1.7103	S14-C55	1.722(13)	1.7221
S9-C37	1.751(11)	1.7325	S15-C64	1.740(12)	1.7084
S10-C37	1.704(10)	1.7109	S16-C64	1.718(11)	1.7329
S11-C46	1.715(12)	1.7216	S17-C73	1.726(11)	1.7101
S12-C46	1.721(11)	1.7191	S18-C73	1.708(11)	1.7397

[a] For labelling scheme see Fig. 4 in the main article.

Table S2. Some experimental (Expt.) and CASTEP calculated (Calc.) bond angles (°) of polymorph I.[a]

Bond angle	Expt.	Calc.	Bond	Expt.	Calc.
Bi1			Bi4		
S1-C1-S2	118.3(5)	118.61	S19-C82-S20	116.7(7)	118.48
S3-C10-S4	120.3(6)	120.52	S21-C91-S22	120.3(6)	120.58
S6-C19-S5	118.8(6)	118.92	S23-C100-S24	118.4(6)	118.82
S1-Bi1-S2	60.28(7)	60.21	S19-Bi4-S20	60.90(8)	60.42
S3-Bi1-S4	64.94(8)	64.96	S21-Bi4-S22	65.13(8)	65.06
S5-Bi1-S6	65.15(8)	64.94	S23-Bi4-S24	65.07(8)	64.78
Bi1-S1-C1	78.2(3)	77.92	Bi4-S20-C82	81.2(4)	83.00
Bi1-S2-C1	85.1(3)	83.72	Bi4-S19-C82	88.0(4)	80.31
Bi1-S3-C10	91.2(3)	90.31	Bi4-S21-C91	91.6(4)	90.02
Bi1-S4-C10	83.5(3)	84.19	Bi4-S22-C91	86.7(4)	84.33
Bi1-S5-C19	88.6(3)	88.32	Bi4-S23-C100	89.5(4)	88.56
Bi1-S6-C19	87.0(3)	87.55	Bi4-S18-C73	95.3(3)	98.60
Bi2			Bi3		
S7-C28-S8	117.7(6)	118.75	S17-C73-S18	120.8(6)	119.16
S9-C37-S10	119.4(6)	119.58	S15-C64-S16	119.0(6)	120.01
S11-C46-S12	120.7(6)	119.83	S13-C55-S14	119.1(7)	119.60
S7-Bi2-S8	62.65(8)	62.11	S17-Bi3-S18	62.55(8)	61.99
S9-Bi2-S10	63.90(8)	63.81	S15-Bi3-S16	64.46(8)	64.20
S11-Bi2-S12	63.43(8)	63.37	S13-Bi3-S14	63.64(8)	63.71
Bi2-S7-C28	85.7(4)	86.17	Bi3-S18-C73	85.5(3)	86.93
Bi2-S8-C28	91.4(4)	91.15	Bi3-S17-C73	90.0(3)	91.01
Bi2-S11-C46	89.3(4)	88.63	Bi3-S14-C55	90.3(4)	89.12
Bi2-S12-C46	85.6(4)	86.94	Bi3-S13-C55	86.8(4)	87.33
Bi2-S9-C37	91.7(3)	90.97	Bi3-S15-C64	92.3(4)	90.88
Bi2-S10-C37	84.8(3)	85.40	Bi3-S16-C64	84.1(4)	84.83
Bi1-S1-Bi2	87.46(7)	87.42	Bi3-S18-Bi4	86.79(7)	87.67
Bi1-S7-Bi2	88.83(7)	89.20	Bi3-S19-Bi4	84.99(7)	85.57

[a] For labelling scheme see Fig. 4 in the main article.

Table S3. Some selected experimental (Expt.) and calculated (Calc.) bond lengths of polymorph II compared with the corresponding bond lengths of II[s].

Polymorph II [a]			Polymorph II[s] [b]		
Bond	Expt.	Calc.	Bond	Expt.	Calc.
Bi1-S11	2.582(2)	2.6304	Bi1-S6	2.561(3)	2.6235
Bi1-S12	2.834(2)	2.8204	Bi1-S5	2.805(3)	2.8070
Bi1-S21	2.806(3)	2.8336	Bi1-S3	2.781(3)	2.8263
Bi1-S22	2.906(3)	2.9014	Bi1-S4	2.888(3)	2.8873
Bi1-S31	2.878(3)	2.9133	Bi1-S1	2.852(3)	2.8991
Bi1-S32	2.790(3)	2.8150	Bi1-S2	2.765(2)	2.8020
S11-C1	1.736(9)	1.7383	S6-C19	1.73(1)	1.7362
S12-C1	1.695(10)	1.7130	S5-C19	1.68(1)	1.7132
S21-C2	1.730(11)	1.7213	S3-C10	1.70(1)	1.7186
S22-C2	1.691(11)	1.7207	S4-C10	1.69(1)	1.7211
S31-C3	1.702(10)	1.7282	S1-C1	1.68(1)	1.7249
S32-C3	1.720(10)	1.7171	S2-C1	1.709(7)	1.7171
C1-N1	1.345(10)	1.3490	C19-N3	1.31(1)	1.3464
C2-N2	1.341(12)	1.3566	C10-N2	1.33(2)	1.3543
C3-N3	1.354(12)	1.3532	C1-N1	1.32(2)	1.3504
N1-C11A	1.450(11)	1.4682	N3-C20	1.45(1)	1.4675
N1-C11B	1.450(11)	1.4703			
C11A-C12A	1.536(10)	1.5233	C20-C21	1.57(3)	1.5272
C11B-C12B	1.535(10)	1.5301			
C12A-C13A	1.556(10)	1.5287	C21-C22	1.38(3)	1.5277
C12B-C13B	1.562(10)	1.5330			
C13A-C14A	1.547(10)	1.5240	C22-C27	1.39(3)	1.5233
C13B-C14B	1.543(10)	1.5277			
N1-C15A	1.450(11)	1.4692	N3-C23	1.51(2)	1.4649
N1-C15B	1.450(11)	1.4686			
C15A-C16A	1.549(10)	1.5299	C23-C24	1.39(2)	1.5208
C15B-C16B	1.553(10)	1.5279			
C16A-C17A	1.543(10)	1.5282	C24-C25	1.55(2)	1.5266
C16B-C17B	1.546(10)	1.5258			
C17A-C18A	1.548(10)	1.5224	C25-C26	1.38(3)	1.5207
C17B-C18B	1.551(10)	1.5212			

[a] For labelling scheme see Fig. 5a in the main article.
[b] For labelling scheme see Fig. S2 in the ESI

Table S4. Selected experimental (Expt.) and CASTEP/PBE calculated (Calc.) bond angles (°) of polymorph II compared with the corresponding bond angles in II^s.

Polymorph II			Polymorph II^s		
Bond angle [a]	Expt.	Calc.	Bond angle [b]	Expt.	Calc.
S11–Bi1–S12	66.18(8)	66.23	S5–Bi1–S6	66.32(8)	66.49
S21–Bi1–S22	62.26(9)	62.44	S3–Bi1–S4	62.22(8)	62.75
S31–Bi1–S32	62.70(7)	62.22	S1–Bi1–S2	62.56(7)	62.57
S11–C1–S12	119.6(5)	119.57	S5–C19–S6	119.1(5)	121.43
S21–C2–S22	119.4(6)	119.50	S3–C10–S4	119.4(6)	119.76
S31–C3–S32	119.1(6)	118.49	S1–C1–S2	118.7(6)	118.74
C1–N1–C11A	119(2)	122.61	C19–N3–C23	122.9(9)	122.80
C1–N1–C11B	125.9(18)	122.91			
N1–C11A–C12A	118(2)	115.09	N3–C23–C24	113(1)	115.03
N1–C11B–C12B	108.5(19)	113.32			
C11A–C12A–C13A	114(2)	110.82	C23–C24–C25	106(1)	109.98
C11B–C12B–C13B	104(2)	113.74			
C12A–C13A–C14A	93(2)	113.68	C24–C25–C26	116(2)	113.42
C12B–C13B–C14B	123(2)	114.83			
C1–N1–C15A	119.6(16)	121.57	C19–N3–C20	121.3(9)	121.47
C1–N1–C15B	121.9(19)	120.23			
N1–C15A–C16A	106.2(17)	111.8	N3–C20–C21	110(1)	111.71
N1–C15B–C16B	116(2)	114.44			
C15A–C16A–C17A	128(3)	113.54	C20–C21–C22	128(1)	113.28
C15B–C16B–C17B	95.7(19)	110.29			
C16A–C17A–C18A	108(2)	114.36	C21–C22–C27	91(2)	113.58
C16B–C17B–C18B	97(2)	113.61			

[a] For atom labelling scheme. see Fig. 5a in the main article
[b] For atom labelling scheme. see Fig. S2 in the ESI.

Table S5. Experimental and GIPAW calculated ^{13}C and ^{15}N <mark>isotropic</mark> chemical shift values of polymorph I.

Labels	H-opt	Full-opt	Expt.	Labels	H-opt	Full-opt	Expt.
C1	205.8	207.6	206.1	N1	186.9	178.4	180.8
C82	205.1	206.5	206.1	N2	168.9	190.7	180.8
C73	204.3	206.1	205.4	N3	177.0	188.6	180.8
C28	203.1	204.7	205.4	N4	184.6	173.6	180.8
C19	203.3	204.2	202.3	N5	179.3	187.4	180.2
C100	205.0	203.4	202.3	N6	183.0	184.1	180.2
C46	203.1	203.5	201.4	N7	187.6	182.8	178.0
C55	199.5	202.3	201.4	N8	185.1	186.5	178.0
C37	202.6	203.5	201.1	N9	181.3	170.9	174.4
C64	201.2	201.1	201.1	N10	186.9	177.8	174.4
C10	198.6	201.0	200.2	N11	187.1	190.8	169.1
C91	198.0	200.4	200.2	N12	193.3	188.5	169.1
-N-CH_2-	62.1	59.0	55.7	-CH_2-CH_3	23.5	22.0	21.9
	60.5	57.7	55.7		23.0	21.5	21.9
	59.7	57.4	55.7		22.5	21.3	21.5
	59.6	56.9	55.7		22.3	21.3	21.5
	58.9	56.9	55.5		22.3	21.2	21.1
	58.8	56.5	55.5		22.3	21.1	21.1
	58.6	56.2	55.1		22.2	21.0	21.1
	58.3	55.9	55.1		21.7	20.5	21.1
	58.0	55.9	54.7		21.4	20.1	21.1
	57.8	55.8	54.7		21.2	20.1	21.1
	57.7	55.7	54.7		20.9	20.0	21.1
	57.1	55.7	54.7		20.4	19.9	21.1
	56.9	55.0	54.7		20.1	19.9	21.1
	55.6	53.1	54.7		20.0	19.4	21.1
	55.4	53.0	54.0		19.4	19.3	21.1
	55.2	52.9	54.0		19.3	19.2	21.1
	54.9	51.9	54.0		19.1	19.2	21.1
	54.6	51.7	54.0		18.9	19.2	21.1
	54.2	51.5	53.7		18.6	19.0	21.1
	53.6	50.7	53.7		18.1	18.9	21.1
	53.4	50.1	53.7		18.1	18.7	21.1
	51.9	48.6	53.7		17.6	17.3	21.1
	50.2	47.4	52.7		16.6	15.8	20.4
	49.9	47.1	52.7		16.3	15.8	20.4
-CH_2-CH_2-	38.9	31.0	31.6	-CH_3	15.7	15.7	16.8
	33.8	30.3	31.6		15.5	14.9	16.8
	31.5	30.3	30.9		14.9	14.7	15.9
	31.2	30.1	30.9		14.6	14.5	15.9
	30.7	30.1	30.6		14.5	14.5	15.4
	30.6	29.2	30.6		14.5	14.1	15.4
	30.4	29.1	30.6		13.9	13.9	15.0
	30.3	29.0	30.6		13.5	13.7	15.0
	30.2	28.7	30.6		13.4	13.4	15.0
	30.2	28.6	30.6		13.1	13.2	15.0
	30.0	27.9	29.6		13.0	12.5	15.0
	29.4	27.3	29.6		13.0	12.3	15.0
	29.3	26.9	29.6		12.5	12.2	14.7
	28.3	26.9	29.6		12.1	11.8	14.7
	27.4	26.6	29.3		11.9	11.7	14.7
	26.9	26.3	29.3		11.9	11.4	14.7

26.8	26.3	29.2	11.4	11.1	14.7
26.3	26.2	29.2	11.2	10.9	14.7
26.0	26.0	29.2	10.9	10.8	14.1
25.7	24.9	29.2	10.9	10.3	14.1
25.6	23.9	28.9	10.9	9.8	13.8
25.4	23.2	28.9	10.0	9.7	13.8
24.7	22.6	28.7	9.1	15.7	13.8
24.6	22.1	28.7	9.0	14.9	13.8

**Table S6.** GIPAW calculated ^{13}C and ^{15}N isotropic chemical shifts values for polymorph II and II^s.

Labels	H-opt[a]	Full-opt[a]	H-opt-A[b]	H-opt-B[b]	Full-opt-A[b]	Full-opt-B[b]	Expt.[b]
C1	191.4	199.9	198.7	194.4	201	201.5	204.7
C2	193.1	203.2	199.5	198.6	205.3	204.7	203.6
C3	196.1	204.4	204.4	210.3	204.3	206.8	199.9
-NCH$_2$-	72.5	59.8	62.6	69.0	59.4	61.7	56.6
	63.0	57.7	55.9	65.4	56.1	61.2	56.6
	61.1	56.2	53.3	63.4	55.6	59.2	55.8
	59.9	54.7	53.1	63.0	54.2	55.9	54.9
	57.1	54.3	49.8	59.0	53.8	54.6	54.2
	49.4	51.3	44.4	54.3	50.4	53.3	53.6
-CH$_2$-	42.8	30.7	38.6	39.9	30.6	31.7	30.8
	34.8	30.2	36.3	35.8	30.3	29.3	30.5
	32.9	28.0	33.4	31.3	28.3	29.3	30.5
	30.8	27.1	33.2	30.9	27.8	28.8	29.6
	30.4	27.1	32.9	30.1	26.6	26.9	29.1
	28.1	25.3	26.8	28.7	26.1	26.7	28.8
-CH$_2$-	25.9	22.7	23.7	24.5	22.3	21.9	21.6
	25.8	20.6	23.7	24.0	20.7	20.5	21.3
	25.2	20.4	22.9	23.3	20.5	20.2	21.3
	24.1	19.6	22.5	22.6	20.3	19.6	20.9
	20.9	19.6	21.2	22.2	19.5	18.2	20.8
	19.5	19.6	18.9	20.9	19.0	18.2	20.8
-CH$_3$	15.7	17.5	18.5	15.7	16.2	14.9	15.5
	15.4	16.0	17.2	15.2	15.9	14.1	15.5
	14.8	15.8	16.6	13.9	15.3	13.8	15.4
	13.9	14.2	16.0	13.7	13.1	13.5	15.1
	9.9	11.5	15.7	13.2	12.7	13.4	14.2
	8.4	11.3	14.0	12.6	10.5	10.1	14.2
N2	157.3	169.8	163.5	162.4	169.6	169.9	177.3
N3	195.4	174.9	174.1	165.7	175.5	175.8	171.2
N1	172.6	176.9	174.9	179.2	177.3	177.6	167.7

[a] Polymorph II^s. Original crystal structure was taken from Sun *et al*. [29]. The atom labelling scheme has been modified for easy comparison with polymorph II (Atom labelling scheme: C3=C1, C2=C10, C1=C19, N1=N3, N2=N2, and N3=N1, see Fig. 5a in the main article).
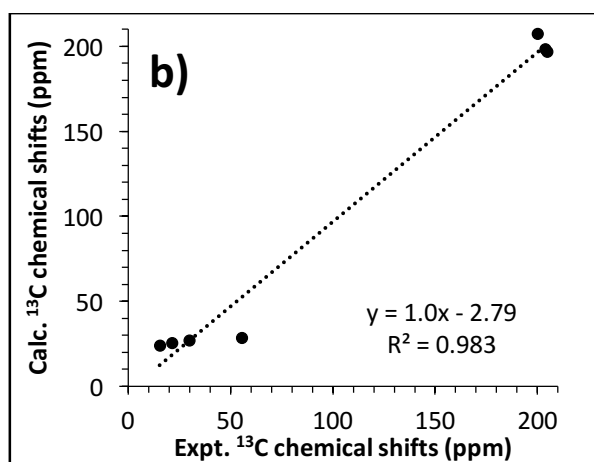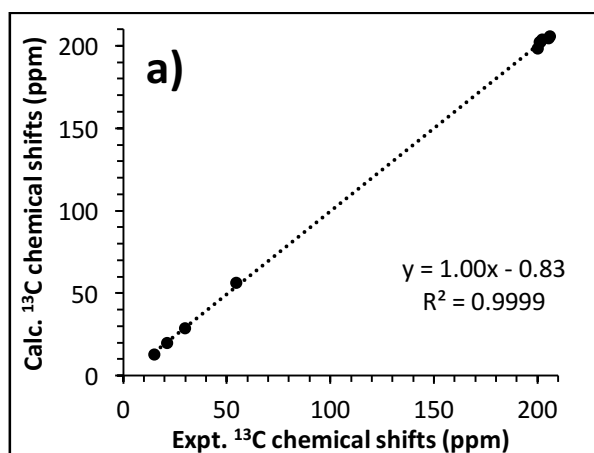[b] Polymorph II.

a)

b)
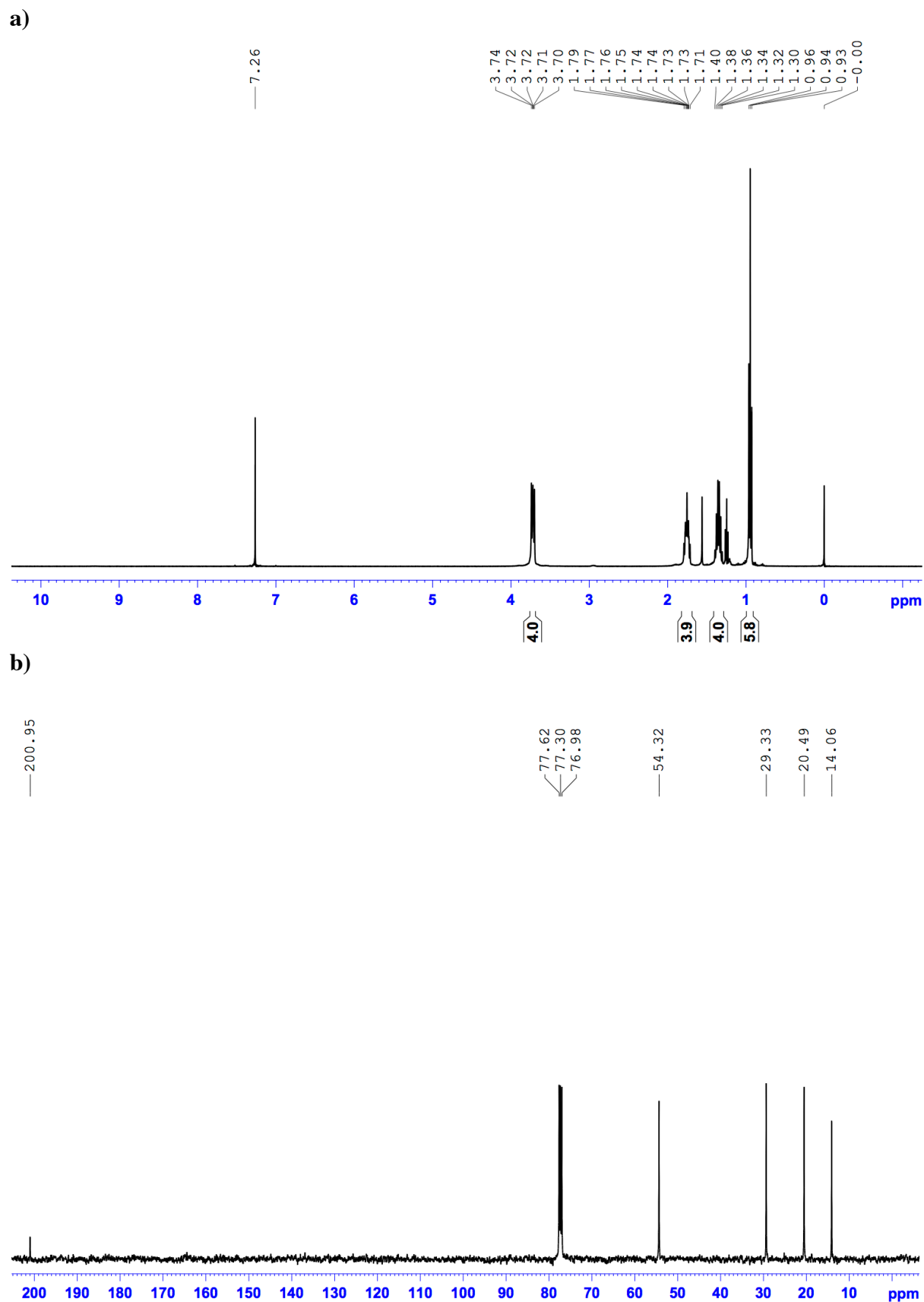
Figure S1. 400 MHz ^{1}H (**a**) and 100 MHz ^{13}C NMR (**b**) spectra of [Bi$_1${S$_2$CN(n-C$_4$H$_9$)$_2$}$_3$] complex in CDCl$_3$ solution.
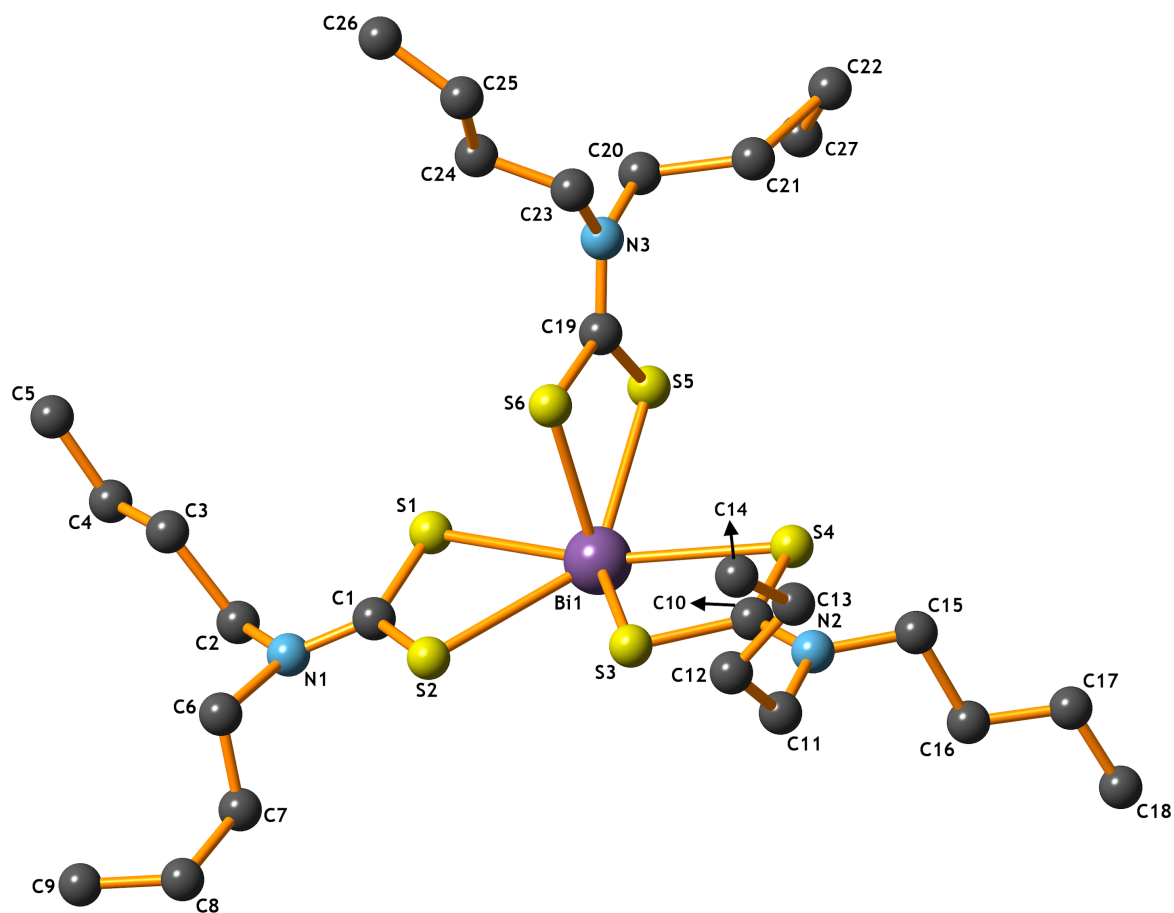
Figure S2. The mononuclear structure and atom labelling scheme of polymorph IIs with the atoms drawn as shaded spheres (anisotropic atomic displacement parameters (ADP) are missing in the reported crystal structure data by Sun *et al.*).
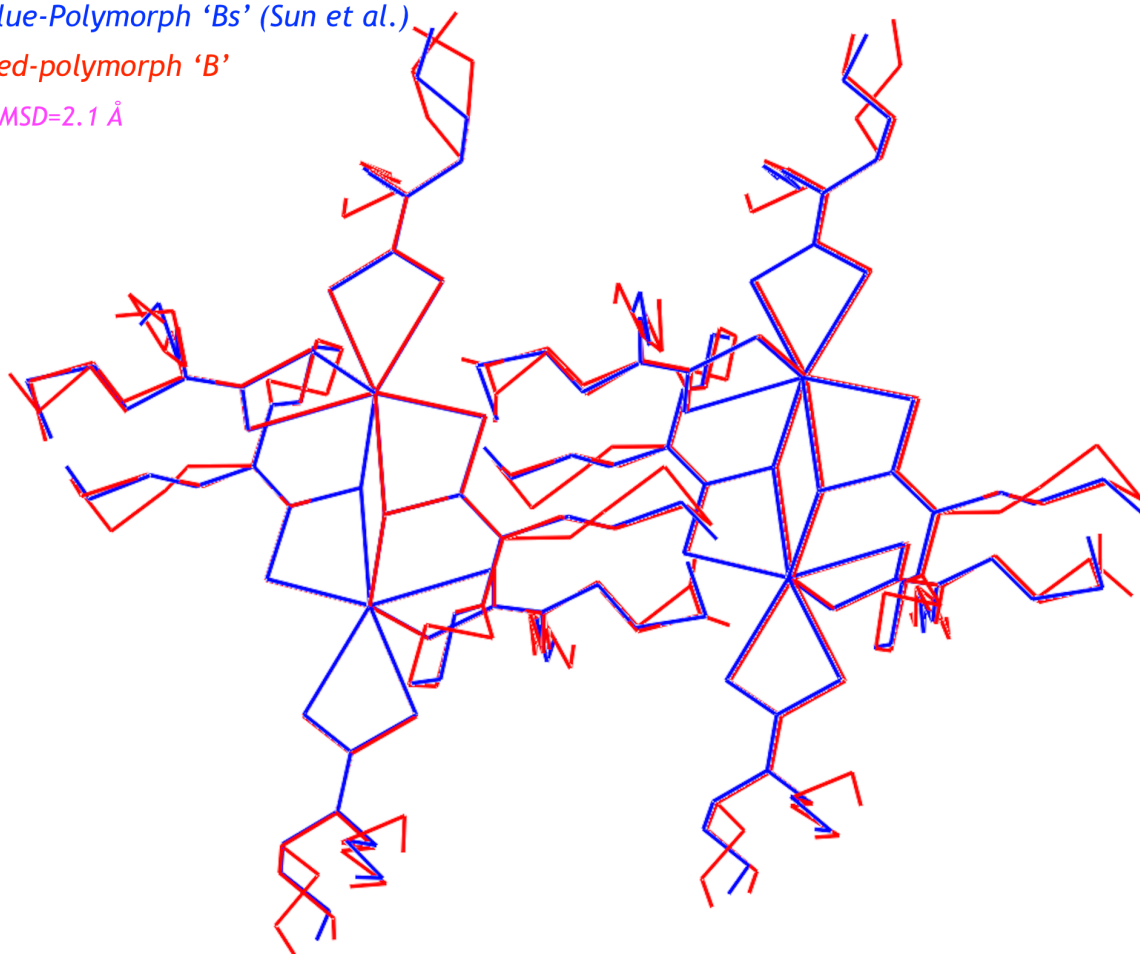
Figure S3. Linear regression plots of calculated and experimental ^{13}C chemical shifts for the "H-opt" structures of (**a**) polymorph I and (**b**) polymorph II. The ^{13}C shieldings were converted into chemical shifts using a reference value of 170.9 ppm.

Blue-Polymorph 'Bs' (Sun et al.)
Red-polymorph 'B'
RMSD=2.1 Å

Figure S4. The structural superposition of the centrosymmetric dimers of polymorph II (blue) and IIs (red). For clarity. the H atoms are not shown here.

Red - "full-opt" - polymorph 'Bs'

Black -"full-opt" - polymorph 'B'- A conformer

Blue -"full-opt" - polymorph 'B'- B conformer

RMSD (heavy atoms): 'Bs' and A-conformer = 0.06 Å
'Bs' and B-conformer = 1.3 Å

Figure S5. The superposition of the "full-opt" molecular structures of IIs and the two conformers of polymorph II. For clarity. the H atoms are omitted.